

A comparison of the clinopyroxene compounds $\text{CaZnSi}_2\text{O}_6$ and $\text{CaZnGe}_2\text{O}_6$

Günther J. Redhammer^{a*} and G. Roth^b

^aDivision of Mineralogy and Materials Science, Department of Geography, Geology and Mineralogy, University of Salzburg, Hellbrunnerstrasse 34, A-5020 Salzburg, Austria, and ^bInstitute of Crystallography, Technical University of Aachen, Jägerstraße 17/19, D-52056 Aachen, Germany
Correspondence e-mail: guenther.redhammer@aon.at

Received 27 October 2004

Accepted 14 December 2004

Online 15 January 2005

Single crystals of $\text{CaZnSi}_2\text{O}_6$ (calcium zinc silicate) and $\text{CaZnGe}_2\text{O}_6$ (calcium zinc germanate) were synthesized at 1623 K and 2.5 GPa by slow cooling of the melts from 1473 K. Structure solution using Patterson methods revealed the two compounds to be isomorphous and thus isostructural. They adopt the clinopyroxene structure type with space group $C2/c$. The substitution of Ge^{4+} for Si^{4+} increases the distortion of the tetrahedra and octahedra. The increased size of the tetrahedral GeO_4 chain is mainly compensated by (i) increasing the kinking of the tetrahedral chain and (ii) lengthening the $\text{Zn}-\text{O}$ bonds.

Comment

The title compounds belong to the common clinopyroxene structure type with a general structural formula of $M2M1T_2O_6$ (M and T are octahedral and tetrahedral cations, respectively). Several of the most important Fe- and Mg-bearing rock-forming minerals occur within this mineral group, among them $\text{CaFeSi}_2\text{O}_6$ (hedenbergite) and $\text{CaMgSi}_2\text{O}_6$ (diopside). $\text{CaZnSi}_2\text{O}_6$ (petedunnite) is one of the less common clinopyroxene minerals and was first described by Essene & Peacor (1987), who only reported the lattice parameters. The three-dimensional crystal structure was determined later from a synthetic sample (Ohashi *et al.*, 1996). We present here a new refinement of the crystal structure of synthetic $\text{CaZnSi}_2\text{O}_6$ and compare the results with the analogous germanate, $\text{CaZnGe}_2\text{O}_6$, whose structure has been determined for the first time.

$\text{CaZnSi}_2\text{O}_6$ and $\text{CaZnGe}_2\text{O}_6$ are isomorphous and thus isostructural. They crystallize in space group $C2/c$ at room temperature and adopt the general structural topology of the clinopyroxenes. This consists of infinite chains of corner-sharing TO_4 tetrahedra ($T = \text{Si}^{4+}$ or Ge^{4+}) running parallel to the c axis, zigzag chains of edge-sharing M1O_6 octahedra

($M1 = \text{Zn}^{2+}$) and eight-coordinate $M2$ sites hosting Ca^{2+} ions (Fig. 1, and Tables 1 and 2). A more detailed discussion and a polyhedral representation of the clinopyroxene structure type is given by Clark *et al.* (1969), Cameron & Papike (1981) and, more recently, Redhammer & Roth (2004).

The average $M1-\text{O}$ bond length in $\text{CaZnSi}_2\text{O}_6$ is smaller than that in $\text{CaFeSi}_2\text{O}_6$ but larger than that in CaMSi_2O_6 ($M = \text{Ni}, \text{Mg}$ and Co ; Table 3), reflecting the differences in $M1$ ionic radii. The distortion parameters, however, do not exhibit a common trend. Among the calcium silicate clinopyroxenes, the Zn^{2+} compound shows the largest bond-length distortion (BLD) and a large octahedral angle variance (Table 3). The $M1$ octahedra in $\text{CaZnSi}_2\text{O}_6$ and $\text{CaCoSi}_2\text{O}_6$ can be readily compared, as both compounds have similar $M1$ ionic radii and almost identical average $M1-\text{O}$ bond lengths (Table 3). The large distortion of the $M1$ octahedron in $\text{CaZnSi}_2\text{O}_6$ corresponds to a (4+2)-coordination by oxygen and is consistent with the fact that the Zn^{2+} ion is more commonly found in tetrahedral coordination. Replacing Si^{4+} by Ge^{4+} causes a distinct increase of the $\text{Zn}-\text{O}$ bond lengths, a doubling of the octahedral angle variance and an increase in bond- and edge-length distortion (Table 3). The largest increase in bond length upon $\text{Si}^{4+}/\text{Ge}^{4+}$ substitution occurs for the $\text{Zn}-\text{O1}(-x, 1-y, -z)$ bond, which is aligned parallel to the c axis. The stretching of this bond reflects the increased size of the tetrahedral chain, also running along the c axis.

The Ca^{2+} ion at the $M2$ site is in an eightfold coordination in the calcium clinopyroxene series, and there is no large structural change either upon changing the $M1$ cation or upon replacing Si^{4+} by Ge^{4+} . The tetrahedron in $\text{CaZnSi}_2\text{O}_6$ is the same within experimental error as in other calcium silicate

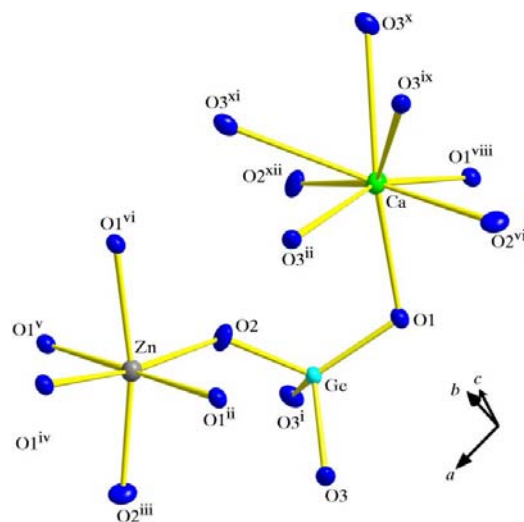


Figure 1

Part of the $\text{CaZnGe}_2\text{O}_6$ structure at 298 K, with displacement ellipsoids drawn at the 90% probability level. [Symmetry codes: (i) $x, -y, \frac{1}{2} + z$; (ii) $\frac{1}{2} - x, \frac{1}{2} - y, -z$; (iii) $1 - x, y, \frac{1}{2} - z$; (iv) $\frac{1}{2} + x, \frac{1}{2} + y, z$; (v) $\frac{1}{2} + x, \frac{1}{2} - y, \frac{1}{2} + z$; (vi) $\frac{1}{2} - x, \frac{1}{2} - y, \frac{1}{2} - z$; (vii) $-\frac{1}{2} + x, \frac{1}{2} - y, -\frac{1}{2} + z$; (viii) $-x, y, \frac{1}{2} - z$; (ix) $-\frac{1}{2} + x, \frac{1}{2} + y, z$; (x) $-\frac{1}{2} + x, \frac{1}{2} - y, \frac{1}{2} + z$; (xi) $\frac{1}{2} - x, \frac{1}{2} + y, \frac{1}{2} - z$; (xii) $\frac{1}{2} - x, \frac{1}{2} - y, 1 - z$.]

clinopyroxenes. The distortion parameters are quite large and show that the SiO_4 tetrahedra exhibit large deviations from ideal geometry, e.g. a large tetrahedral angle variance (TAV), mostly as a result of an elongation along the a axis (angle τ in Table 3). In all calcium clinopyroxenes, the tetrahedral chains are kinked to accommodate the size difference between the $M1$ octahedra and the tetrahedra. In $\text{CaZnSi}_2\text{O}_6$, the tetrahedral bridging angle [$165.3(1)^\circ$] compares well with that in $\text{CaCoSi}_2\text{O}_6$ but is smaller than that in $\text{CaMgSi}_2\text{O}_6$. A decrease of this bridging angle with increasing size of the $M1$ cation can be observed (Table 3).

The replacement of Si^{4+} by Ge^{4+} in the Zn^{2+} clinopyroxene results in an increase of the average $T\text{—O}$ bond length by 0.122 \AA , which is close to the difference in ionic radius between Si^{4+} and Ge^{4+} (0.14 \AA ; Shannon & Prewitt, 1969). The GeO_4 tetrahedron appears to be more elongated along the a axis, resulting in a tetrahedral angle variance that is almost twice as large (Table 3). The tetrahedral bridging angle decreases from $165.3(1)^\circ$ in the silicate to $158.5(1)^\circ$ in the germanate in order to match the larger GeO_4 tetrahedra to the chain of ZnO_6 octahedra. Obviously this mechanism is not sufficient, since a distinct lengthening of the Zn—O bonds is also observed. Finally, the increase of the average $T\text{—O}$ bond length is not as large as might be expected from the ionic radii alone. Besides increasing the kinking of the tetrahedral chains and the Zn—O bond length, this can be seen as a third mechanism to maintain size compatibility between the tetrahedral and octahedral chains.

Our lattice parameters of $\text{CaZnSi}_2\text{O}_6$ are similar to those given in the literature (Essene & Peacor, 1987; Ohashi *et al.*, 1996; Huber *et al.*, 2004). The latter authors have determined the lattice parameters of petedunnite, but no additional structure information. The substitution of Ge^{4+} for Si^{4+} causes an increase of the unit-cell volume by 8.3%, which is mainly due to a lengthening of the a and c parameters by $3.78(0.37 \text{ \AA})$ and $3.54\%(0.19 \text{ \AA})$, respectively. The b lattice parameter increases only slightly (0.35%). The small expansion along b can be explained by the increased kinking of the tetrahedral chain in the germanate structure. As the tetrahedral chains run parallel to the c axis and the tetrahedral apices point towards the a axis, the large expansions of the unit cell along these directions directly reflect the replacement of Si^{4+} by Ge^{4+} .

Experimental

The starting materials were prepared by mixing CaCO_3 , ZnO , and SiO_2 or GeO_2 in the exact stoichiometry of the compounds. The oxide mixture of $\text{CaZnSi}_2\text{O}_6$ was placed in a small Pt tube (5 mm long, inner diameter 3 mm), which was welded tight at both ends and transferred to the piston-cylinder apparatus of the Institute of Crystallography, RWTH Aachen. The synthesis was performed at 1623 K and 2.5 GPa, and yielded small transparent crystals up to $100 \mu\text{m}$ in size with a short prismatic habit. $\text{CaZnGe}_2\text{O}_6$ was produced by slow cooling from the melt. The starting material was placed in an open Pt crucible and heated slowly to 1473 K. This temperature was maintained for 24 h before cooling slowly to 1073 K at a rate of 0.5 K min^{-1} . Large crystals of up to 1 mm in size were recovered.

Compound (I)

Crystal data

$\text{CaZnSi}_2\text{O}_6$
 $M_r = 257.63$
 Monoclinic, $C2/c$
 $a = 9.7955(8) \text{ \AA}$
 $b = 8.9781(8) \text{ \AA}$
 $c = 5.251(6) \text{ \AA}$
 $\beta = 106.033(7)^\circ$
 $V = 443.8(5) \text{ \AA}^3$
 $Z = 4$

$D_x = 3.856 \text{ Mg m}^{-3}$
 Mo $K\alpha$ radiation
 Cell parameters from 1256 reflections
 $\theta = 2.1\text{--}28.2^\circ$
 $\mu = 7.18 \text{ mm}^{-1}$
 $T = 298(1) \text{ K}$
 Cuboid, colourless
 $0.08 \times 0.07 \times 0.06 \text{ mm}$

Data collection

Stoe IPDS-I diffractometer
 φ scans
 Absorption correction: numerical
 via equivalents ($X\text{-SHAPE}$ and
 $X\text{-RED}$; Stoe & Cie, 1996)
 $T_{\text{min}} = 0.56$, $T_{\text{max}} = 0.66$
 2095 measured reflections

527 independent reflections
 445 reflections with $I > 2\sigma(I)$
 $R_{\text{int}} = 0.029$
 $\theta_{\text{max}} = 28.1^\circ$
 $h = -12 \rightarrow 12$
 $k = -11 \rightarrow 11$
 $l = -6 \rightarrow 6$

Refinement

Refinement on F^2
 $R[F^2 > 2\sigma(F^2)] = 0.021$
 $wR(F^2) = 0.058$
 $S = 1.05$
 527 reflections
 48 parameters

$w = 1/[\sigma^2(F_o^2) + (0.0364P)^2 + 0.1449P]$
 where $P = (F_o^2 + 2F_c^2)/3$
 $(\Delta/\sigma)_{\text{max}} = 0.001$
 $\Delta\rho_{\text{max}} = 1.52 \text{ e \AA}^{-3}$
 $\Delta\rho_{\text{min}} = -0.58 \text{ e \AA}^{-3}$
 Extinction correction: $SHELXL97$
 Extinction coefficient: 0.0095 (9)

Table 1

Selected geometric parameters (\AA , $^\circ$) for (I).

Zn—O1^{ii}	2.070 (3)	Ca—O3^{ii}	2.739 (2)
Zn—O2	2.0739 (18)	Si—O2	1.5850 (19)
Zn—O1^{iv}	2.1613 (19)	Si—O1	1.600 (2)
$\text{Ca—O2}^{\text{iii}}$	2.325 (3)	Si—O3^{i}	1.684 (2)
Ca—O1	2.3512 (19)	Si—O3	1.670 (2)
Ca—O3^{xi}	2.601 (2)		
$\text{O1}^{\text{ii}}\text{—Zn—O2}$	89.39 (8)	O2—Si—O1	117.10 (10)
$\text{O1}^{\text{iv}}\text{—Zn—O2}$	92.52 (8)	$\text{O2—Si—O3}^{\text{i}}$	103.70 (10)
$\text{O2—Zn—O2}^{\text{iii}}$	94.03 (10)	$\text{O1—Si—O3}^{\text{i}}$	109.76 (10)
$\text{O1}^{\text{ii}}\text{—Zn—O1}^{\text{iv}}$	84.78 (8)	O2—Si—O3	110.14 (10)
$\text{O1}^{\text{iv}}\text{—Zn—O1}^{\text{iv}}$	93.08 (8)	O1—Si—O3	110.90 (10)
$\text{O2}^{\text{iii}}\text{—Zn—O1}^{\text{iv}}$	92.88 (7)	$\text{O3}^{\text{i}}\text{—Si—O3}$	104.25 (9)
$\text{O1}^{\text{iv}}\text{—Zn—O1}^{\text{xi}}$	80.82 (10)	$\text{Si}^{\text{xi}}\text{—O3—Si}$	135.84 (13)

Symmetry codes: (i) $x, -y, z + \frac{1}{2}$; (ii) $-x + \frac{1}{2}, -y + \frac{1}{2}, -z$; (iii) $-x + 1, y, -z + \frac{1}{2}$; (iv) $x + \frac{1}{2}, y + \frac{1}{2}, z$; (v) $x + \frac{1}{2}, -y + \frac{1}{2}, z + \frac{1}{2}$; (vi) $x - \frac{1}{2}, -y + \frac{1}{2}, z - \frac{1}{2}$; (vii) $x - \frac{1}{2}, y + \frac{1}{2}, -z + \frac{1}{2}$; (viii) $x, -y, z - \frac{1}{2}$.

Compound (II)

Crystal data

$\text{CaZnGe}_2\text{O}_6$
 $M_r = 346.63$
 Monoclinic, $C2/c$
 $a = 10.1659(8) \text{ \AA}$
 $b = 9.0096(7) \text{ \AA}$
 $c = 5.4369(4) \text{ \AA}$
 $\beta = 105.181(4)^\circ$
 $V = 480.59(6) \text{ \AA}^3$
 $Z = 4$

$D_x = 4.791 \text{ Mg m}^{-3}$
 Mo $K\alpha$ radiation
 Cell parameters from 1520 reflections
 $\theta = 2.1\text{--}28.2^\circ$
 $\mu = 18.40 \text{ mm}^{-1}$
 $T = 298(2) \text{ K}$
 Cuboid, colourless
 $0.15 \times 0.12 \times 0.11 \text{ mm}$

Data collection

Stoe IPDS-I diffractometer
 φ scans
 Absorption correction: numerical
 via equivalents ($X\text{-SHAPE}$ and
 $X\text{-RED}$; Stoe & Cie, 1996)
 $T_{\text{min}} = 0.079$, $T_{\text{max}} = 0.135$
 1919 measured reflections

572 independent reflections
 532 reflections with $I > 2\sigma(I)$
 $R_{\text{int}} = 0.040$
 $\theta_{\text{max}} = 28.2^\circ$
 $h = -13 \rightarrow 13$
 $k = -11 \rightarrow 10$
 $l = -7 \rightarrow 7$

Table 2

Selected geometric parameters (Å, °) for (II).

Ca—O2 ⁱⁱⁱ	2.3687 (19)	Zn—O1 ^{iv}	2.177 (2)
Ca—O1	2.370 (2)	Ge—O2	1.713 (2)
Ca—O3 ⁱⁱ	2.633 (2)	Ge—O1	1.721 (2)
Ca—O3 ^{xi}	2.679 (2)	Ge—O3	1.788 (2)
Zn—O2	2.076 (2)	Ge—O3 ⁱ	1.809 (2)
Zn—O1 ⁱⁱ	2.100 (2)		
O2—Zn—O2 ⁱⁱⁱ	100.94 (12)	O2—Ge—O1	118.29 (10)
O2—Zn—O1 ⁱⁱ	91.32 (8)	O2—Ge—O3	109.14 (10)
O2 ⁱⁱⁱ —Zn—O1 ⁱⁱ	88.45 (7)	O1—Ge—O3	112.31 (9)
O2 ⁱⁱⁱ —Zn—O1 ^{iv}	89.43 (8)	O2—Ge—O3 ⁱ	101.66 (9)
O1 ⁱⁱ —Zn—O1 ^{iv}	83.90 (8)	O1—Ge—O3 ⁱ	112.98 (9)
O1 ^v —Zn—O1 ^{iv}	96.37 (7)	O3—Ge—O3 ⁱ	100.55 (6)
O1 ^{iv} —Zn—O1 ^{xi}	80.72 (11)	Ge—O3—Ge ^{xiii}	128.54 (11)

Symmetry codes: (i) $x, -y, z + \frac{1}{2}$; (ii) $-x + \frac{1}{2}, -y + \frac{1}{2}, -z$; (iii) $-x + 1, y, -z + \frac{1}{2}$; (iv) $x + \frac{1}{2}, y + \frac{1}{2}, z$; (v) $x + \frac{1}{2}, -y + \frac{1}{2}, z + \frac{1}{2}$; (vii) $x - \frac{1}{2}, -y + \frac{1}{2}, z - \frac{1}{2}$; (xi) $-x + \frac{1}{2}, y + \frac{1}{2}, -z + \frac{1}{2}$; (xiii) $x, -y, z - \frac{1}{2}$.

Refinement

Refinement on F^2

$$R[F^2 > 2\sigma(F^2)] = 0.025$$

$$wR(F^2) = 0.057$$

$$S = 1.07$$

572 reflections

48 parameters

$$w = 1/[\sigma^2(F_o^2) + (0.0389P)^2]$$

$$\text{where } P = (F_o^2 + 2F_c^2)/3$$

$$(\Delta/\sigma)_{\max} < 0.0001$$

$$\Delta\rho_{\max} = 1.11 \text{ e } \text{Å}^{-3}$$

$$\Delta\rho_{\min} = -0.88 \text{ e } \text{Å}^{-3}$$

Extinction correction: *SHELXL97*

Extinction coefficient: 0.0352 (13)

A second crystal of CaZnGe₂O₆ was investigated by single-crystal X-ray diffraction and gave atomic coordinates and structural parameters that are the same within experimental error. Lattice parameters for CaZnGe₂O₆ were also refined from a powder (obtained by crushing several single crystals), using whole pattern fitting, and are the same as those from the single-crystal data within experimental error.

For both compounds, data collection: *X-Area* (Stoe & Cie, 2002); cell refinement: *X-Area*; data reduction: *X-Area*; structure solution: *SHELXS97* (Sheldrick, 1997); structure refinement: *SHELXL97* (Sheldrick, 1997); molecular graphics: *DIAMOND* (Brandenburg & Berndt, 1999); publication software: *WinGX* (Farrugia, 1999).

GJR thanks the Austrian Science Foundation (Fonds zur Förderung der wissenschaftlichen Forschung, FWF) for financial support through an ‘Erwin-Schrödinger-Rückkehr-Stipendium’ grant No. R33-N10.

Supplementary data for this paper are available from the IUCr electronic archives (Reference: BC1062). Services for accessing these data are described at the back of the journal.

Table 3

Structural and distortional parameters for selected calcium clinopyroxenes.

Sample	CaMgSi ₂ O ₆ ^a	CaCoSi ₂ O ₆ ^b	CaZnSi ₂ O ₆ ^c	CaFeSi ₂ O ₆ ^d	CaZnGe ₂ O ₆ ^e
$\langle M2-O \rangle$ (Å)	2.498	2.502	2.504	2.511	2.513
BLD _{M2} ^e (%)	5.81	6.46	6.63	6.48	5.70
Volume (Å ³)	25.76	25.52	25.92	26.10	26.52
$\langle M1-O \rangle$ (Å)	2.077	2.101	2.102	2.130	2.118
BLD _{M1} ^e (%)	1.47	1.13	1.89	1.35	1.87
ELD _{M1} ^f (%)	2.89	2.83	2.70	2.48	3.37
OAV _{M1} ^g (°)	17.75	14.66	18.54	14.96	33.67
e_u/e_{sM1} ^h	1.041	1.028	1.057	1.022	1.071
Volume (Å ³)	11.86	12.28	12.28	12.81	12.47
$\langle T-O \rangle$ (Å)	1.636	1.635	1.635	1.635	1.758
BLD _T ^e (%)	2.51	2.40	2.58	2.54	2.32
ELD _T ^f (%)	1.36	1.43	1.37	1.41	2.65
TAV _T ⁱ (°)	26.77	25.52	24.29	24.78	47.73
τ^j (°)	112.66	112.69	112.59	112.63	114.53
Volume (Å ³)	2.23	2.23	2.22	2.22	2.74
$r(M1)^k$	0.72	0.735	0.745	0.78	0.745

Notes: (a) diopside (Sasaki *et al.*, 1980); (b) Ghose *et al.* (1987); (c) this study; (d) hedenbergite (Clark *et al.*, 1969); (e) bond-length distortion (BLD) = $(100/n) \sum_{i=1}^n \{ |(X-O)_i - \langle X-O \rangle| / \langle X-O \rangle \}$, where n is the number of bonds, $\langle X-O \rangle$ is the central cation-oxygen length and $\langle X-O \rangle$ is the average cation-oxygen bond length (Renner & Lehmann, 1986); (f) edge-length distortion (ELD) = $(100/n) \sum_{i=1}^n \{ |(O-O)_i - \langle O-O \rangle| / \langle O-O \rangle \}$, where n is the number of edges, $\langle O-O \rangle$ is the polyhedron edge length and $\langle O-O \rangle$ is the average polyhedron edge length (Renner & Lehmann, 1986); (g) octahedral angle variance (OAV) = $\sum_{i=1}^n (\Theta_i - 90) / 11$ (Robinson *et al.*, 1971); (h) unshared edge e_u /shared edge e_s (Toraya, 1981); (i) tetrahedral angle variance (TAV) = $\sum_{i=1}^n (\Theta_i - 109.47) / 5$ (Robinson *et al.*, 1971); (j) τ is the mean of the three $O_{\text{basal}}-T-O_{\text{apex}}$ angles; (k) ionic radius (Shannon & Prewitt, 1969).

References

Brandenburg, K. & Berndt, M. (1999). *DIAMOND*. Version 2.1b. Crystal Impact GbR, Bonn, Germany.
 Cameron, M. & Papike, J. J. (1981). *Am. Mineral.* **66**, 1–50.
 Clark, J. R., Appleman, E. E. & Papike, J. J. (1969). *Mineral. Soc. Am. Spec. Pap.* **2**, 31–50.
 Essene, E. J. & Peacor, D. R. (1987). *Am. Mineral.* **72**, 157–166.
 Farrugia, L. J. (1999). *J. Appl. Cryst.* **32**, 837–838.
 Ghose, S., Wan, C. & Okamura, F. P. (1987). *Am. Mineral.* **72**, 375–381.
 Huber, A. L., Heuer, M., Fehr, K. T., Bente, K., Schmidbauer, E. & Bromiley, G. D. (2004). *Phys. Chem. Minerals*, **31**, 67–79.
 Ohashi, H., Osawa, T., Sato, A. & Tsukimura, K. (1996). *J. Min. Pet. Econ. Geol.* **91**, 21–27.
 Redhammer, G. J. & Roth, G. (2004). *Z. Kristallogr.* **219**, 278–294.
 Renner, B. & Lehmann, G. (1986). *Z. Kristallogr.* **175**, 43–59.
 Robinson, K., Gibbs, G. V. & Ribbe, P. H. (1971). *Science*, **172**, 567–570.
 Sasaki, S., Fujino, K., Takeuchi, Y. & Sadanaga, R. (1980). *Acta Cryst.* **A36**, 904–915.
 Shannon, R. D. & Prewitt, C. T. (1969). *Acta Cryst.* **B25**, 925–934.
 Sheldrick, G. M. (1997). *SHELXL97* and *SHELXS97*. University of Göttingen, Germany.
 Stoe & Cie (1996). *X-SHAPE* and *X-RED*. Stoe & Cie, Darmstadt, Germany.
 Stoe & Cie (2002). *X-Area*. Stoe & Cie, Darmstadt, Germany.
 Toraya, H. (1981). *Z. Kristallogr.* **157**, 173–190.